

000
001
002054
055
056

Enhancing Social Relation Inference with Concise Interaction Graph and Discriminative Scene Representation

003
004
005
006
007057
058
059
060
061008 Anonymous ICCV submission
009
010
011
012
013
014
015062
063
064
065
066016 Paper ID 8211
017
018
019
020
021
022
023
024
025
026
027
028
029
030
031
032
033
034
035
036
037
038067
068
069
070
071
072
073
074

Abstract

There has been a recent surge of research interest in attacking the problem of social relation inference based on images. Existing works classify social relations mainly by creating complicated graphs of human interactions, or learning the foreground and/or background information of persons and objects, but ignore holistic scene context. The holistic scene refers to the functionality of a place in images, such as dining room, playground and office. In this paper, by mimicking human understanding on images, we propose an approach of **P**RACTical **I**nference in **S**ocial **r**Elation (**PRISE**), which concisely learns interactive features of persons and discriminative features of holistic scenes. Technically, we develop a simple and fast relational graph convolutional network to capture interactive features of all persons in one image. To learn the holistic scene feature, we elaborately design a contrastive learning task based on image scene classification. To further boost the performance in social relation inference, we collect and distribute a new large-scale dataset, which consists of about 240 thousand unlabeled images. The extensive experimental results show that our novel learning framework significantly beats the state-of-the-art methods, e.g., **PRISE** achieves 6.8% improvement for domain classification in PIPA dataset.

039
040
041083
084
085

1. Introduction

042
043
044
045
046
047
048
049
050
051
052
053086
087
088
089
090
091
092
093
094
095
096
097
098
099

Social relations describe the connections among two or more individuals, which are fundamental to daily life of human beings [17]. Nowadays, billions of people share images in social media platforms such as Facebook and Twitter. In light of [3], common social relations include family, couple, friends, colleagues, professional, etc. There has been an increasing interest in understanding social relations among persons from still images due to the broad applications including group behavior analysis [13], image caption generation [15] and human trajectory prediction [1].

The problem of social relation inference is challenging

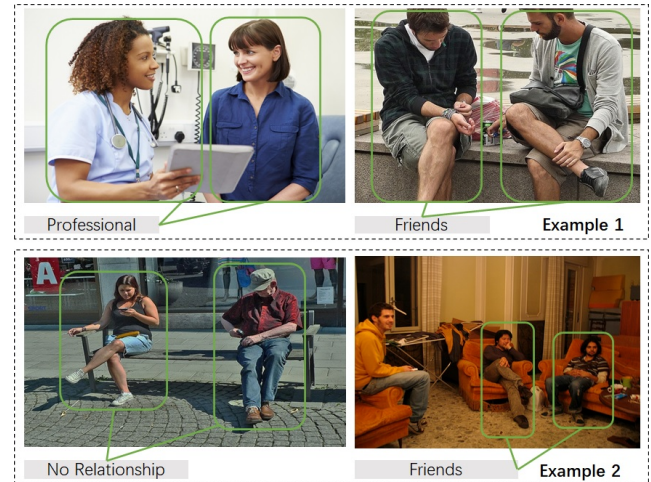


Figure 1. The comparison of inferring social relations under different scenes, with images taken from PISC dataset [19]. Example 1 shows relations of professional and friends corresponding to hospital and park, respectively. Example 2 significantly implies a close relation in the context of staying indoors.

and complicated because it requires high-level semantic understanding of images. Inspired by the cognition process of human beings on images, we summarize three steps for classification of social relations. First, we take a whole view of the scene, which represents the functionality of a place. Second, we identify the background objects and persons, and the foreground union regions of person pair in images. Third, we observe the interaction of persons, such as hugging and handshaking. With these information in mind, we infer the category of relationships for all persons.

To demonstrate the importance of scene at inferring social relations, we present two examples in Figure 1. Each example consisting of two images shows different relationships mainly due to the scene context. For instance, Example 1 shows the professional relationship in the context of hospital and the relationship of friends in the context of a park. It is clear that the scene information should be carefully taken into consideration for social relation inference.

108 We note that prior works put more effort into learning
109 from human interactions, the foreground union regions of
110 person pair, and the background information of persons and
111 objects, but missed the importance of holistic scene context,
112 especially in inferring relationships from different scenes
113 with similar human interactions. Goel et al. [10] adopted
114 a pre-trained model to directly output the feature of fore-
115 ground regions, which missed the whole context and may
116 get a less representative feature. Zhang et al. [34] utilized
117 a pre-trained model with ImageNet to generate a feature at
118 the level of object classification. The resultant feature can-
119 not semantically summarize high-level scene features.
120

121 A large number of studies proposed models to learn so-
122 cial relations based on interaction graph of persons in an
123 image [10, 20, 29, 34]. Wang et al. [29] proposed graphs
124 of persons and objects to infer social relations. The signifi-
125 cant drawback of [29] is that graphs of persons and objects
126 can only characterize the connection between two persons,
127 which leads to complicated calculations for cases of three
128 or more persons in an image.

129 It is urgent and essential to attack the problem of social
130 relation inference in a broader view where an interaction
131 graph works for two or more persons and simultaneously
132 the scene feature provides holistic hints for the classifica-
133 tion of relationships. In this paper, inspired by the under-
134 standing process of human beings, we propose an approach of
135 **P**Ractical **I**nference in **S**ocial **r**Elation (PRISE), which syn-
136 thetizes three streams of information, i.e., holistic scenes,
137 foreground and background information of persons and ob-
138 jects, and interaction of persons. To the best of our knowl-
139 edge, we are the first to methodically and systematically de-
140 velop a model to learn the holistic scene feature in social
141 relation inference based on contrastive learning.

142 In PRISE, we first technically design a concise relational
143 graph convolutional network (RGCN) to extract the interac-
144 tive features of all persons in one image. Then, to boost the
145 performance in social relation inference, a contrastive learn-
146 ing task for capturing holistic scene is incorporated into the
147 proposed PRISE. Intuitively, the contrastive learning task
148 helps to extract discriminative features of the holistic scene
149 context. We demonstrate that PRISE achieves a significant
150 improvement in social relation inference compared to the
151 state-of-the-art methods.

152 We summarize our contributions in this work as follows.

- 153 • We systematically develop a novel approach, i.e.,
154 PRISE, for social relation classifications. PRISE sig-
155 nificantly beats the state-of-the-art methods in social
156 relation inference.
- 157 • We design a concise relational graph convolutional
158 network to capture the interactive features for all per-
159 sons. The proposed RGCN is simpler and faster than
160 the graph model in [20].

- 162 • We construct a contrastive learning task to learn dis-
163 criminative representation of holistic scene. We dis-
164 tribute a new large-scale dataset for contrastive learn-
165 ing, which is named as PISC-extension. The useful-
166 ness of PISC-extension can be extended to other tasks
167 in computer vision, such as group behaviour analysis.
168
- 169 • Extensive experiments including a comprehensive ab-
170 lation study demonstrate the effectiveness the PRISE,
171 and show the significance of interaction graph and
172 scene information in social relation inference.
173

2. Related Work

174 To assess our contributions in classification of social re-
175 lations, it is important to consider three streams of studies:
176 social relation inference, graph neural networks and con-
177 trastive learning.

2.1. Social Relation Inference

178 For a large number of scenarios in computer vision, so-
179 cial information has played an important role by providing
180 additional cues in tasks of image understanding, e.g., hu-
181 man interaction [26], kinship recognition [22, 21, 23] and
182 image caption generation [31].

183 The pioneering work on social relation inference dates
184 back to 2010 from [28], where the authors developed a
185 model to characterize the interaction between multi-person
186 actions, facial appearances and identities. Zhang et al. [37]
187 developed a deep neural network to learn social relation
188 traits from rich facial attributes, such as expression, gen-
189 der, and age. In [37], the social relation traits were defined
190 based on psychological studies [12, 11], consisting of eight
191 types, e.g., trusting and friendly.

192 For datasets in social relations, Zhang et al. [35] dis-
193 tributed a dataset to evaluate classification of social rela-
194 tions, which is named as People In Photo Albums (PIPA).
195 Besides, another dataset, which is People in Social Context
196 (PISC), was published in [19].

197 With PIPA and PISC, several interesting works move for-
198 ward along the research line of social relation understand-
199 ing [27, 29, 10, 20]. In light of domain based theory from
200 social psychology, Sun et al. [27] presented a model with
201 semantic attributes to classify social relations and domains.
202 Wang et al. [28] modelled a knowledge graph with proper
203 messages propagation and attention to learn the social re-
204 lations among people in an image. Recently, in [10], Goel
205 et al. proposed an end-to-end neural network to learn the
206 interaction graph of persons. In [20], a social graph was
207 proposed to restrict logical connections of persons, which
208 achieved the state-of-the-art results in social relation infer-
209 ence. In Table 1, we present the differences between our
210 PRISE and the prior studies in terms of feature information.

216 Table 1. Comparisons between our PRISE and previous methods
 217 in features for social relation inference. “Fore.” is short for “Foreground” and “Back.” is short for “Background”.
 218

Methods	Interaction Graph	Fore. & Back.	Holistic Scene
Pair CNN [19]	No	Yes	No
Dual-Glance [19]	No	Yes	No
SRG-GN [10]	Yes	Yes	No
GRM [29]	Yes	Yes	No
MGR [34]	Yes	Yes	No
GR ² N [20]	Yes	No	No
PRISE	Yes	Yes	Yes

2.2. Graph Neural Networks

Inspired by the success of convolutional networks in the computer vision domain, GNNs are proposed to re-define the notation of convolution for graph structured data [16]. Most recently, GNNs have been adopted to social relation reasoning [29, 34, 20]. For instance, Zhang et al. [34] designed person-object graph and person-pose graph, and conducted social relation reasoning on these two graphs by GNN. Li et al. [20] proposed a graph relational reasoning network to jointly infer social relations by building a graph for each image, where the nodes represent the persons and the edges represent the relations. In this paper, we follow the similar graph-based approach proposed in [20], and design a concise relational graph convolutional network to extract interactive features among people in the image.

2.3. Contrastive Learning

Over the last few years, contrastive representation learning based on deep learning models has shown the power in many practical tasks [4, 6, 7, 24, 30, 33, 36], especially for natural language and computer vision domains. Contrastive learning usually maximizes similarity and dissimilarity over data samples which are organized into similar and dissimilar pairs, respectively.

A significant challenge in contrastive learning is how to select the similar (or positive) and dissimilar (or negative) pairs. The main difference among different approaches of contrastive learning lies in their strategy for obtaining sample pairs [5]. To generate sample pairs without additional human labels, many researchers create models with multiple views of each sample. Besides, for complicated tasks, some studies also construct positive and negative sample pools from pre-trained models [9, 18]. In this paper, by utilizing the pseudo-labels from a pre-trained model of image scene classification, we construct negative and positive sample pools, and design a contrastive learning task to learn discriminative scene representations.

3. Methodology

In this section, we first introduce the approach that converts all persons in an image into an interaction graph, and then apply the RGCN model on the graph to learn interactive features of people in the same image. Finally, to better utilize scene information for social relation understanding, we propose a contrastive learning approach to learn discriminative scene representation. The overall pipeline of PRISE is shown in Figure 2.

3.1. Graph-based Approach

Inspired by [20], we adopt graph-based approach. We build a graph for each image, where each person in an image is modeled as a node in the graph. The edge between two nodes represents the social relation between the corresponding two persons. For simplicity, we consider the fully connected graph, i.e., each pair of persons in the image has an edge. Denote $\mathcal{G} = (\mathcal{V}, \xi)$ as the fully connected graph with node set \mathcal{V} and edge set ξ in an image.

For each image, we extract three types of features using a ImageNet pre-trained model (i.e., ResNet101). These three types of features include RoI features of single person, union region of person pairs (a.k.a. foreground feature), and persons and objects of the whole image (a.k.a background feature). In the following, we will introduce the detailed ways to generate these features.

Following traditional approach in detection, the feature representation of each person is extracted directly from the last convolutional feature map of the input image. Specifically, given input image I with N bounding boxes b_1, b_2, \dots, b_N for N persons, we obtain the feature representations of all people in the image using a pre-trained ResNet101 model, where an RoI pooling layer is constructed based on the last convolutional feature map. Note that the RoI pooling layer is a common trick in social relation learning with graph representation [20]. Denote the feature representation of the i -th person in image I as x_i ,

$$x_i = f_{CNN-RoI}(I, b_i) \in \mathbb{R}^F, i = 1, 2, \dots, N, \quad (1)$$

where $F = 2048$ is the feature dimension for each person. For simplicity, we denote the set of feature representations for people in image I as $X = \{x_1, x_2, \dots, x_N\}$.

In addition, we obtain the features of union regions of person pair using the same approach. For person i and j , we first compute the bounding box of their union region b_{ij} . Then we get its feature as follows:

$$x_{ij} = f_{CNN-RoI}(I, b_{ij}). \quad (2)$$

Besides, we also obtain x_I , the feature representation for the whole image, by setting the bounding box to cover the whole image and passing it to $f_{CNN-RoI}$.

$$x_I = f_{CNN-RoI}(I, b_I), \quad (3)$$

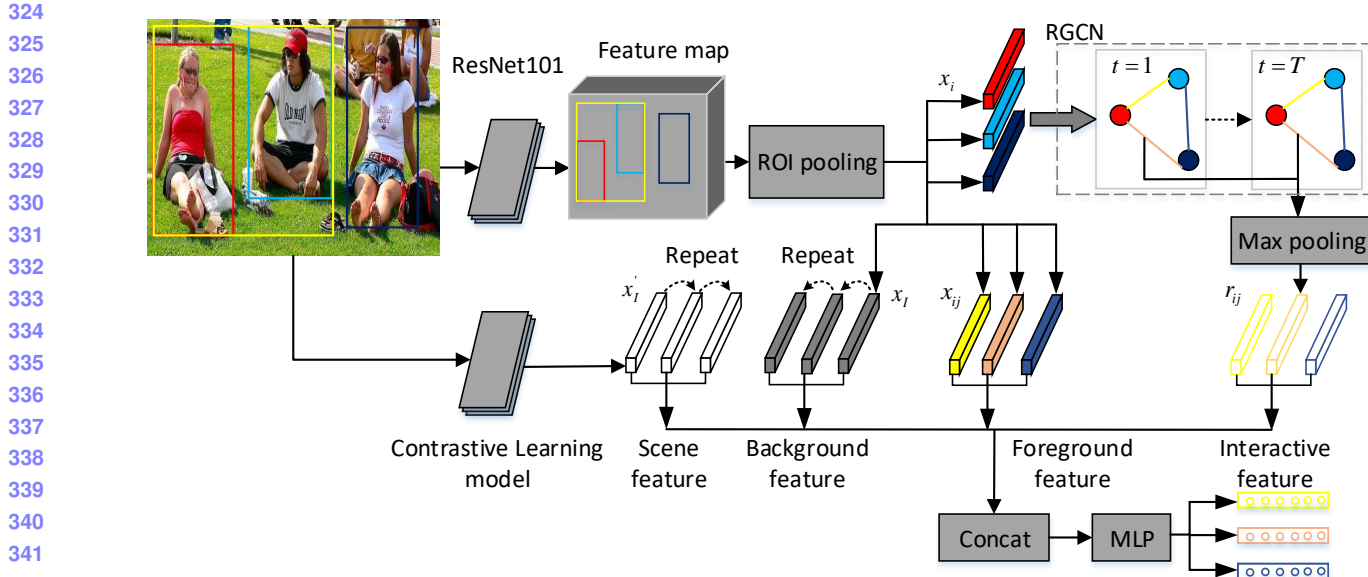


Figure 2. The overall pipeline of PRISE model. Given an input image I , we use ResNet101 to extract ROI features of people in the image x_i , foreground feature x_{ij} and background feature x_I . In addition, another pre-trained ResNet50 that was finetuned using contrastive learning approach to extract discriminative scene feature x'_I . The RGCN is used to obtain interactive feature between person pair r_{ij} . Finally, $r_{ij}, x_I, x_{ij}, x'_I$ are concatenated and passed to a MLP layer for relation classification. The network outputs relational class distribution for all person pairs in the image. The operation ‘Repeat’ is a must to keep the number of scene and background features the same as the number of person pairs when there exist more than two persons in an image.

where b_I is the bounding box for the whole image. Intuitively, the feature of single person x_i encodes personalized information of each person, the feature of union region x_{ij} encodes the pair-wise foreground information, while the feature of whole image x_I encodes the background of all persons and objects. Thus, all these features can provide useful information for social relation understanding.

3.2. Relational Graph Convolutional Network

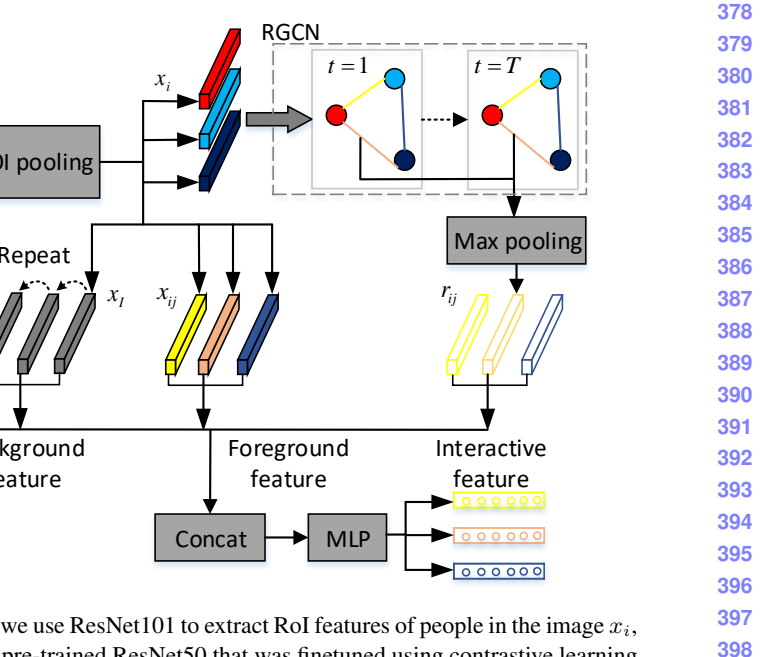
In this section, we introduce RGCN, an end-to-end trainable network architecture, that can learn pair-wise interactive features given arbitrary graph structured data. We apply RGCN on the fully connected graph \mathcal{G} with features X .

Given \mathcal{G} and X , for each node $i \in \mathcal{V}$, we set its initial node feature vectors as $h_i^0 = wx_i \in \mathbb{R}^F, \forall i \in \mathcal{V}$, where $w \in \mathbb{R}^{F \times F}$ is a learnable parameter that maps input feature vectors to the new feature space. Correspondingly, each edge has a feature vector, and we denote the initial edge feature vector between node i and node j as $r_{ij}^0 \in \xi$. In RGCN with T layer, the edge and node feature vectors are updated iteratively for T times. Specifically, at t -th layer the edge and node representations can be expressed as follows:

$$r_{ij}^t = \sigma(W^t h_i^t + W^t h_j^t), \quad (4)$$

$$h_i^{t+1} = h_i^t + \sigma(W^t h_i^t + \sum_{j \in \mathcal{N}_i} r_{ij}^t \odot W^t h_j^t), \quad (5)$$

where \mathcal{N}_i is the set of neighbors for node i , $W^t \in$



$\mathbb{R}^{F \times F}, t = 1, 2, \dots, T$ are the learnable parameters at each layer, and $\sigma(\cdot)$ is the ReLU function.

We note that the RGCN defined in (4)-(5) is an anisotropic variant of GCN [8]. Similar to Residual GateGCN [2], our RGCN has residual connections on the node feature representations, and explicitly maintains edge feature at each layer. Intuitively, the edge feature representations at different layers encode the pair-wise human interaction information. Following similar ideas in JK-Net [32], we obtain the final interactive features by using a max pooling on the edge representations from different RGCN layers. Formally, the final interactive feature between person i and j , denoted as r_{ij} , can be expressed as

$$r_{ij} = f_{max}(r_{ij}^0, r_{ij}^1, \dots, r_{ij}^T), \quad (6)$$

where $f_{max}(\cdot)$ is an element-wise max function.

3.3. Discriminative Scene Representation Learning

The scene of an image provides important visual clues for social relation understanding. For instance, given a party scene, the group of people are more likely to be friends than colleagues, and a group of athletes running on a track are much more likely to be sports team members than band members [10]. To harvest the power of pre-trained CNN model and unlimited amount of unlabeled images, in this paper, we propose a contrastive learning (CL) approach for discriminative scene representation learning.

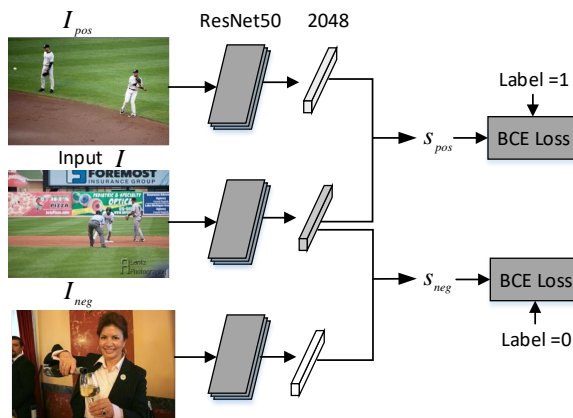


Figure 3. An overview structure of CL task. For a given image I , we first sample a similar image I_{pos} and a dissimilar image I_{neg} from the image dataset. All these three images are passed through the pre-trained ResNet50 model to obtain a feature representation.

Following the CL paradigm, we design a scene classification task to distinguish between similar and dissimilar images. As a pre-process step, we use the pre-trained ResNet50 model [38] to obtain the top-5 scene classes for each unlabeled image. Two images are defined as similar in scene if there are more than K scene classes that are the same among the top-5 scene classes. Otherwise, they are dissimilar. Based on this definition, we can have for each image a pool of similar images and a pool of dissimilar images. The structure of CL task is shown in Figure 3. For each input image I , we randomly sample one image I_{pos} from its pool of similar images to construct positive sample, and another image I_{neg} from its pool of dissimilar images to construct negative sample. We then apply the pre-trained ResNet50 model on these three images I, I_{pos}, I_{neg} to extract features, denoted as $x, x_{pos}, x_{neg} \in \mathbb{R}^F$, respectively. The similarity scores of samples are calculated using a simple bilinear scoring function with sigmoid activation function as follows:

$$s_{pos} = \sigma(xWx_{pos}), \quad s_{neg} = \sigma(xWx_{neg}),$$

where $W \in \mathbb{R}^{F \times F}$ is learnable parameter, σ is the sigmoid function. The pre-trained ResNet50 model is finetuned using the binary cross-entropy loss function. Namely, the loss function can be expressed as

$$L_{cl} = \frac{1}{|I|} \sum_I (-\log(s_{pos}) - \log(1 - s_{neg})). \quad (7)$$

We note that the structure of the CL task is similar to Triplet network [14]. Intuitively, the task is designed to map images with similar scenes closely to each other and dissimilar scenes separable as farther apart as possible. Thus images with similar scenes could have high similarity scores

and vice versa. This contrastive learning paradigm enables the model to learn discriminative scene representations.

After finetuning the pre-trained CNN model, we use it as a scene feature extractor in our downstream social relation inference task. Namely, given an image I , we obtain the scene feature of the image as follows:

$$x'_I = f_{CL-RoI}(I, b_I), \quad (8)$$

where $f_{CL-RoI}(\cdot)$ represents the CL finetuned CNN model with RoI pooling layer.

Finally, to predict the relational class distribution of person i and j in the image, we concatenate their interactive feature r_{ij} extracted from RGCN model, foreground feature x_{ij} , background feature x_I extracted from ImageNet pre-trained CNN model and discriminative scene feature x'_I extracted from CL finetuned model together. The concatenated features are fed as input to the MLP layer for relation classification. The network outputs relational class distribution for all person pairs in the image.

We note that most of the previous methods, such as Pair CNN, Dual-Glance, SRG-GN, etc, consider the social relations on the same image separately. Namely, their model outputs relational class distribution for single pair of person *only*, even if there are multiple people in the image. This may cause occurrence of some obviously unreasonable and contradictory relationships in one image. In contrast, our model directly learns the joint distribution of social relations for multiple people. Given an image as input, PRISE extracts features of multiple people in the image and directly outputs the relational class distributions for *all* person pairs. This enables our model to generate reasonable and consistent social relationships in one image.

4. Experiments

In this section, we conduct extensive experiments based on PIPA and PISC, as well as a new large-scale unlabeled dataset. We first present the description of datasets and the implementation details. Then we evaluate the performance of our proposed model through comparisons with benchmarks and ablation study. Finally, we visualize the results from the CL model with discussions. All the codes and experimental results are publicly available on github¹.

4.1. Datasets

Social Relation Datasets. We conduct experiments on two social relation datasets, i.e., the PIPA dataset [35] and the PISC dataset [19]. The *accuracy* over all classes is used to evaluate all methods in PIPA dataset. The PISC dataset has a hierarchy of three coarse-level relations (intimate, non-intimate, no relation) and six fine-level relations (friend, family, couple, professional, commercial, and no relation).

¹<https://github.com/IFBigData/PRISE>

540 Table 2. Comparisons of the accuracy (in %) between our PRISE
 541 and other state-of-the-art methods in PIPA dataset.

Methods	domain	relation
Pair CNN [19]	65.9	58.0
Dual-Glance [19]	-	59.6
SRG-GN [10]	-	53.6
GRM [29]	-	62.3
MGR [34]	-	64.4
GR ² N [20]	72.3	64.3
PRISE	77.2	69.5

552 For fair comparisons, we follow the standard train/val/test
 553 split in [19]. The *per-class recalls* and *mean Average Precision*
 554 (*mAP*) are used to evaluate all methods in PISC dataset.

555 **Contrastive Learning Dataset.** For CL, we extend PISC
 556 dataset to a new dataset with 240,200 images by using
 557 google image search engine. Specifically, we search for 10
 558 similar images on Google for every image in PISC dataset,
 559 thus extending PISC dataset by approximately 10 times. We
 560 combine the extended dataset with PIPA and PISC images
 561 and name it as PISC-extension dataset. We show some ex-
 562 amples from this dataset in supplementary materials. We
 563 take 80% of samples in the PISC-extension dataset as the
 564 training set, and the remaining samples as the test set.

565 4.2. Implementation Details

566 **Contrastive Learning.** We use the pre-trained ResNet50
 567 model [38] to obtain the top-5 scene categories of an input
 568 image. We then construct positive and negative sample
 569 pairs based on the scene category. Each image has a pool of
 570 positive samples and a pool of negative samples. For sim-
 571 plicity, we limit the maximum number of images in a pool
 572 for each image. In this paper, we set the maximum num-
 573 ber as 50². In the training phase, we randomly select one
 574 image from the positive and negative sample pool respec-
 575 tively. We set the batch size to be 32, the learning rate to be
 576 1×10^{-5} . The ResNet50 model is finetuned end-to-end
 577 using the Adam optimizer. For the performance of the fine-
 578 tuned ResNet50 model, the accuracy and AUC on the test
 579 set are 91.0% and 96.7%, respectively. After training, the
 580 network parameters are saved for the downstream task.

581 **Training of PRISE.** Our PRISE is trained with a learning
 582 rate of 5×10^{-5} . We resize the input image into 448×448 ,
 583 and train the network for 20 epochs with a batch size of 32.
 584 The number of layers in RGCN is set to be 2, i.e., $T = 2$.

585 4.3. Comparisons with Benchmarks

586 In experiments, we compare PRISE with the following
 587 existing methods. For fair comparisons, we report the best

588 ²We have considered other values (e.g., 30, and 80) and found that this
 589 parameter is insensitive to the results.

590 results in experiments for Tables 2 and 3 following the rou-
 591 tine in this research field.

592 **Pair CNN** [19]. Two cropped image patches of the two
 593 persons are fed into two CNNs with sharing weights to ex-
 594 tracted features for social relation classification.

595 **Dual-Glance** [19]. The first glance focuses on the pair
 596 of people. The second glance extracts the information of
 597 objects in the context to refine the prediction.

598 **SRG-GN** [10]. Scene and human attribute context fea-
 599 tures are extracted by five CNNs.

600 **GRM** [29]. This model represents the person and objects
 601 existing in an image as a weighted graph, and then using a
 602 gated graph network to predict social relation.

603 **MGR** [34]. This model employs two graph neural net-
 604 work (GNN) to extract the relationship between people and
 605 the relationship between people and objects.

606 **GR²N** [20]. This model uses GNN to model all rela-
 607 tionships in one graph which can provide strong logical
 608 constraints among different types of social relations.

609 It is worth noting that all of the above methods, except
 610 GR²N, are person pair-based, which means that they con-
 611 sider the pair-wised social relations on the same image sep-
 612 arately. In contrast, both PRISE and GR²N consider the
 613 social relations among all people in one image jointly. Un-
 614 like our method, GR²N do not use foreground, background
 615 and scene features. Besides, Dual-Glance, GRM and MGR
 616 use object information in an image to assist in relation
 617 inference. We note that in SRG-GN, they directly apply the
 618 pre-trained scene classification model as feature extractor
 619 for foreground ground information, while in our PRISE, we
 620 first use the CL approach to finetune the pre-trained model,
 621 and then apply the model for scene feature extraction.

622 The experimental results of social domain recognition
 623 and social relationship recognition in PIPA dataset are
 624 shown in Table 2. We observe that our PRISE outperforms
 625 other methods by a significant margin. Specifically, our
 626 method achieves an accuracy of 77.2% for social domain
 627 recognition and 69.5% for social relation recognition, beat-
 628 ing all the person pair-based methods. This shows the ben-
 629 efit of graph-based approach that jointly models all the so-
 630 cial relationships among people in an image. Besides, our
 631 method improves the current state-of-the-art method, i.e.,
 632 GR²N, by 6.8% for social domain recognition and 8.1% for
 633 social relation recognition, respectively.

634 Similar results can be found in Table 3, where we shows
 635 the experimental comparison with prior methods in PISC
 636 dataset. We observe that our method achieves an mAP of
 637 83.4% for the coarse-level recognition and 73.8% for the
 638 fine-level recognition, which are new state-of-the-art. We
 639 note that PRISE takes full advantage of holistic scene and
 640 thus makes better predictions for non-intimate relation. For
 641 degradation in ‘Int’ and ‘Fri’, we argue that the similar
 642 scenes of ‘Fri’ and ‘Fam’ misleads our model.

648 Compared with GR²N, PRISE achieves competitive performance for both coarse and fine relationship recognition
 649 with a much simpler GCN structure. The above results
 650 highlight the benefits of concise interaction graph and dis-
 651 criminative scene feature in PRISE.
 652
 653

654 4.4. Ablation Study

655 We conduct ablation study to show how much each component of PRISE contributes to the performance. Specifically, we remove the interactive feature, the scene feature, the foreground and background features from PRISE, denoted as *w/o Int.*, *w/o Scene*, *w/o Fore.*, *w/o Back.*, respectively. In addition, to show the effectiveness of discriminative scene representation, we consider a variant denoted by *PRISE|Pretrained*, where we replace the CL finetuned model with the ResNet50 that was pretrained on Place365 dataset. The results are summarized in Table 4.

656 As we can see in Table 4, among all the four components, the interactive feature is the most important, followed by the scene feature. Without interactive feature, the mean of mAP in PISC-coarse and PISC-Fine dataset drops 7.4% and 11.3% in absolute value, respectively. These two numbers become 0.8% and 0.9% if we remove the scene feature from PRISE. On one hand, this result demonstrates the effectiveness of RGCN to extract interactive feature. On the other hand, it shows the benefit of considering scene information in social relation understanding.

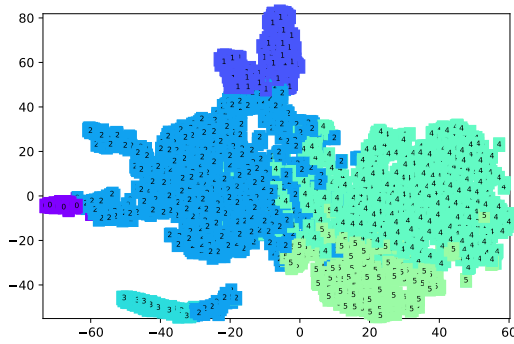
657 Besides, by comparing the results of *PRISE|Pretrained*
 658 and PRISE, we clearly find that the discriminative scene
 659 representation provides significant hints for social relation
 660 classifications, especially for fine relationships with 1.8%
 661 relative improvement.

662 4.5. Visualization of Scene Representations

663 To demonstrate the discriminative scene representation learned by our CL finetuned model, we randomly choose 4000 images from PISC-coarse test dataset, and conduct a clustering task based on the learned features. Specifically, we first use the CL finetuned model to generate the 2048-dimensional scene representations for each image. Then, we use spectral clustering to cluster these features. The 4000 test images are divided into 6 categories. We visualize sample images in different clusters in supplementary materials. We use TSNE to reduce the features dimension from 2048 to 2, and visualize them in Figure 4. We can observe that images from different categories are separated. These results directly show that the features learned by our CL finetuned model are discriminative.

698 4.6. Discussions on Effectiveness of PRISE

700 **RGCN as Interactive Feature Extractor: Simpler and**
 701 **Faster.** We would have used GR²N [20] as the interactive



702
 703
 704
 705
 706
 707
 708
 709
 710
 711
 712
 713
 714
 715
 716
 717
 718
 719
 720
 721
 722
 723
 724
 725
 726
 727
 728
 729
 730
 731
 732
 733
 734
 735
 736
 737
 738
 739
 740
 741
 742
 743
 744
 745
 746
 747
 748
 749
 750
 751
 752
 753
 754
 755

Figure 4. TSNE visualization of image scene features obtained from CL finetuned model on PISC test dataset. Different colors are used to represent clusters of different categories.

feature extractor, however, we note that it is too complicated. For a social relation inference problem with K categories of social relation, GR²N introduced K sets of trainable parameters. In contrast, the number of parameters of our RGCN does not depend on the number of social relation categories, which makes RGCN much simpler.

To further compare GR²N and RGCN as interactive feature extractors in terms of performance and inference time, we conduct experiments by replacing RGCN with GR²N in PRISE while fixing other components. Specifically, in GR²N each category of social relation has a representation. We apply a max pooling operator on representations of different social relations to obtain the interactive feature, and replace r_{ij} in our PRISE with this new interactive feature. We denote this setting as *PRISE|GR²N*. The experimental results on the accuracy and inference time³ on test set of both algorithms in PIPA dataset are shown in Table 5. We can observe that the performance of PRISE|GR²N is comparable to PRISE. However, in terms of inference time, the model with GR²N is much slower as compared to PRISE. These results strongly support our conclusion that the proposed RGCN model as interactive feature extractor is much simpler and faster as compared to GR²N.

Benefits of Utilizing the Scene Information. Scene information is important for social relation understanding. In Figure 5, we visualize two sample images from PISC test dataset, where *PRISE w/o Scene* makes wrong predictions while PRISE makes correct predictions. In this example, people (in the left image) in a home environment tends to have intimate relation, while people (in the right image) in public environment tends to have non-intimate relation. Without scene information, PRISE makes wrong predictions by predicting the two persons in the left image to have non-intimate relation, and the two persons in the right im-

³The inference time reported here does not include the time needed to extract features using ResNet101 model and CL finetuned model.

756 Table 3. Comparisons of the per-class recall for each relationship and the mAP over all relationship (in %) between our PRISE and other
 757 state-of-the-art methods in PISC dataset. Int: Intimate, Non: Non-Intimate, NoR: No Relation, Fri: Friend, Fam: Family, Cou: Couple,
 758 Pro: Professional, Com: Commercial, NoR: No Relation. 810
 811
 812

Methods	Coarse relationships				Fine relationships						
	Int	Non	NoR	mAP	Fri	Fam	Cou	Pro	Com	NoR	mAP
Pair CNN [19]	70.3	80.5	38.8	65.1	30.2	59.1	69.4	57.5	41.9	34.2	48.2
Dual-Glance [19]	73.1	84.2	59.6	79.7	34.4	68.1	76.3	70.3	57.6	60.9	63.2
SRG-GN [10]	-	-	-	-	-	-	-	-	-	-	71.6
GRM [29]	81.7	73.4	65.5	82.8	59.6	64.4	58.6	76.6	39.5	67.7	68.7
MGR [34]	-	-	-	-	64.6	67.8	60.5	76.8	34.7	70.4	70.0
GR ² N [20]	81.6	74.3	70.8	83.1	60.8	65.9	84.8	73.0	51.7	70.4	72.7
PRISE	73.3	79.2	71.8	83.4	47.1	74.7	76.6	73.2	70.3	68.2	73.8

769
 770
 771 Table 4. Ablation study of the PRISE model in PISC dataset. We
 772 report the mean and standard deviation of mAP (in %) among 50
 773 random runs in PISC dataset. 823
 824

Methods	Coarse	Fine
PRISE w/o Int.	75.3 ± 0.2	61.4 ± 0.4
PRISE w/o Scene	81.9 ± 0.3	71.8 ± 0.4
PRISE w/o Fore.	82.2 ± 0.4	71.9 ± 0.5
PRISE w/o Back.	82.5 ± 0.3	72.5 ± 0.4
PRISE Pretrained	82.2 ± 0.4	71.4 ± 0.4
PRISE	82.8 ± 0.3	72.8 ± 0.5

782
 783 Table 5. Comparisons of GR²N and RGCN in PIPA dataset. We
 784 report the accuracy (in %) and inference time. 835
 836

Methods	domain		relation	
	accuracy	time	accuracy	time
PRISE GR ² N	75.6	3.33s	68.1	6.23s
PRISE	77.2	1.91s	69.5	1.82s

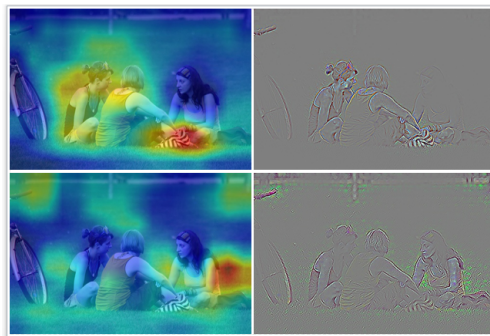
791
 792 age to have intimate relation. More examples are illustrated
 793 in supplementary materials. 845
 846



802 Figure 5. Visualization of sample images from PISC test dataset,
 803 where PRISE w/o Scene makes wrong predictions while PRISE
 804 makes correct predictions. 855
 856

805
 806 Besides, the scene representations extracted from different
 807 models could be very different. In Figure 6, we show
 808 the heat map and gradient map [25] of the pre-trained
 809 models from ImageNet and Place365 [38] dataset, respectively.
 860
 861

813
 814 We can observe that the feature extracted by ImageNet pre-
 815 trained model focuses more on the persons, while the fea-
 816 ture extracted by Place365 pre-trained model focuses more
 817 on the holistic scene. 828
 829



830
 831 Figure 6. Heat map and gradient map of scene representations
 832 extracted from different models. The top two images are the
 833 pre-trained model on Imagenet. The bottom two images are from the
 834 pre-trained model on Place365. 839
 840

5. Conclusion

841
 842 In this paper, we have originally proposed PRISE to en-
 843 hance social relation inference. PRISE synthesizes three
 844 streams of information, i.e., holistic scenes, foreground and
 845 background information of persons and objects, and inter-
 846 action of persons. Technically, we have developed a RGCN
 847 model in PRISE to extract interactive features and designed a CL task
 848 to learn discriminative scene representations. The RGCN
 849 model in PRISE is concise in terms of learning the inter-
 850 action for all persons in an image and the running time of
 851 feature extraction. Extensive experiments demonstrate that
 852 PRISE is superior than prior methods, and achieves new
 853 state-of-the-art results in PIPA and PISC datasets. The con-
 854 trastive learning task in PRISE sheds new lights on improv-
 855 ing performance of more complicated tasks in computer vi-
 856 sion, such as behaviour analysis and image captioning.
 857
 858

864

References

865

866

867

868

869

870

871

872

873

874

875

876

877

878

879

880

881

882

883

884

885

886

887

888

889

890

891

892

893

894

895

896

897

898

899

900

901

902

903

904

905

906

907

908

909

910

911

912

913

914

915

916

917

- [1] Alexandre Alahi, Kratarth Goel, Vignesh Ramanathan, Alexandre Robicquet, Li Fei-Fei, and Silvio Savarese. Social lstm: Human trajectory prediction in crowded spaces. In *Proceedings of the IEEE conference on computer vision and pattern recognition*, pages 961–971, 2016. 1
- [2] Xavier Bresson and Thomas Laurent. Residual gated graph convnets. *ICLR*, 2018. 4
- [3] David G Bromley and Bruce C Busching. Understanding the structure of contractual and covenantal social relations: Implications for the sociology of religion. *SA. Sociological analysis*, pages 15S–32S, 1988. 1
- [4] Ting Chen, Simon Kornblith, Mohammad Norouzi, and Geoffrey Hinton. A simple framework for contrastive learning of visual representations. In *International conference on machine learning*, pages 1597–1607. PMLR, 2020. 3
- [5] Ching-Yao Chuang, Joshua Robinson, Lin Yen-Chen, Antonio Torralba, and Stefanie Jegelka. Debiased contrastive learning. *arXiv preprint arXiv:2007.00224*, 2020. 3
- [6] Jacob Devlin, Ming-Wei Chang, Kenton Lee, and Kristina Toutanova. Bert: Pre-training of deep bidirectional transformers for language understanding. *arXiv preprint arXiv:1810.04805*, 2018. 3
- [7] Carl Doersch, Abhinav Gupta, and Alexei A Efros. Unsupervised visual representation learning by context prediction. In *Proceedings of the IEEE international conference on computer vision*, pages 1422–1430, 2015. 3
- [8] Vijay Prakash Dwivedi, Chaitanya K Joshi, Thomas Laurent, Yoshua Bengio, and Xavier Bresson. Benchmarking graph neural networks. *TSP*, 12:50–500. 4
- [9] Zeyu Feng, Chang Xu, and Dacheng Tao. Self-supervised representation learning from multi-domain data. In *Proceedings of the IEEE/CVF International Conference on Computer Vision*, pages 3245–3255, 2019. 3
- [10] Arushi Goel, Keng Teck Ma, and Cheston Tan. An end-to-end network for generating social relationship graphs. In *Proceedings of the IEEE Conference on Computer Vision and Pattern Recognition*, pages 11186–11195, 2019. 2, 3, 4, 6, 8
- [11] John Gottman, Robert Levenson, and Erica Woodin. Facial expressions during marital conflict. *Journal of Family Communication*, 1(1):37–57, 2001. 2
- [12] Ursula Hess, Sylvie Blairy, and Robert E Kleck. The influence of facial emotion displays, gender, and ethnicity on judgments of dominance and affiliation. *Journal of Nonverbal behavior*, 24(4):265–283, 2000. 2
- [13] Minh Hoai and Andrew Zisserman. Talking heads: Detecting humans and recognizing their interactions. In *Proceedings of the IEEE Conference on Computer Vision and Pattern Recognition*, pages 875–882, 2014. 1
- [14] Elad Hoffer and Nir Ailon. Deep metric learning using triplet network. In *International workshop on similarity-based pattern recognition*, pages 84–92. Springer, 2015. 5
- [15] Mahmoud Khademi and Oliver Schulte. Image caption generation with hierarchical contextual visual spatial attention. In *Proceedings of the IEEE Conference on Computer Vi-*

- sion and Pattern Recognition Workshops*, pages 1943–1951, 2018. 1
- [16] Thomas N. Kipf and Max Welling. Semi-supervised classification with graph convolutional networks. In *ICLR*, 2017. 3
- [17] Shinobu Kitayama and Hazel Rose Markus. The pursuit of happiness and the realization of sympathy: Cultural patterns of self, social relations, and well-being. *Culture and subjective well-being*, 1:113–161, 2000. 1
- [18] Wonhee Lee, Joonil Na, and Gunhee Kim. Multi-task self-supervised object detection via recycling of bounding box annotations. In *Proceedings of the IEEE/CVF Conference on Computer Vision and Pattern Recognition*, pages 4984–4993, 2019. 3
- [19] Junnan Li, Yongkang Wong, Qi Zhao, and Mohan S Kankanhalli. Dual-glance model for deciphering social relationships. In *Proceedings of the IEEE International Conference on Computer Vision*, pages 2650–2659, 2017. 1, 2, 3, 5, 6, 8
- [20] Wanhu Li, Yueqi Duan, Jiwen Lu, Jianjiang Feng, and Jie Zhou. Graph-based social relation reasoning. *arXiv preprint arXiv:2007.07453*, 2020. 2, 3, 6, 7, 8
- [21] Jianqing Liang, Qinghua Hu, Chuangyin Dang, and Wangmeng Zuo. Weighted graph embedding-based metric learning for kinship verification. *IEEE Transactions on Image Processing*, 28(3):1149–1162, 2018. 2
- [22] Jiwen Lu, Junlin Hu, and Yap-Peng Tan. Discriminative deep metric learning for face and kinship verification. *IEEE Transactions on Image Processing*, 26(9):4269–4282, 2017. 2
- [23] Jiwen Lu, Xiuzhuang Zhou, Yap-Pen Tan, Yuanyuan Shang, and Jie Zhou. Neighborhood repulsed metric learning for kinship verification. *IEEE transactions on pattern analysis and machine intelligence*, 36(2):331–345, 2013. 2
- [24] Deepak Pathak, Philipp Krahenbuhl, Jeff Donahue, Trevor Darrell, and Alexei A Efros. Context encoders: Feature learning by inpainting. In *Proceedings of the IEEE conference on computer vision and pattern recognition*, pages 2536–2544, 2016. 3
- [25] Ramprasaath R Selvaraju, Michael Cogswell, Abhishek Das, Ramakrishna Vedantam, Devi Parikh, and Dhruv Batra. Grad-cam: Visual explanations from deep networks via gradient-based localization. In *Proceedings of the IEEE international conference on computer vision*, pages 618–626, 2017. 8
- [26] Xiangbo Shu, Jinhui Tang, Guojun Qi, Wei Liu, and Jian Yang. Hierarchical long short-term concurrent memory for human interaction recognition. *IEEE transactions on pattern analysis and machine intelligence*, 2019. 2
- [27] Qianru Sun, Bernt Schiele, and Mario Fritz. A domain based approach to social relation recognition. In *Proceedings of the IEEE Conference on Computer Vision and Pattern Recognition*, pages 3481–3490, 2017. 2
- [28] Gang Wang, Andrew Gallagher, Jiebo Luo, and David Forsyth. Seeing people in social context: Recognizing people and social relationships. In *European conference on computer vision*, pages 169–182. Springer, 2010. 2
- [29] Zhouxia Wang, Tianshui Chen, Jimmy Ren, Weihao Yu, Hui Cheng, and Liang Lin. Deep reasoning with knowledge

- 972 graph for social relationship understanding. *arXiv preprint arXiv:1807.00504*, 2018. 2, 3, 6, 8 1026
- 973 [30] Tete Xiao, Xiaolong Wang, Alexei A Efros, and Trevor Darrell. What should not be contrastive in contrastive learning. 1027
- 974 *arXiv preprint arXiv:2008.05659*, 2020. 3 1028
- 975 [31] Kelvin Xu, Jimmy Ba, Ryan Kiros, Kyunghyun Cho, Aaron Courville, Ruslan Salakhudinov, Rich Zemel, and Yoshua 1029
- 976 Bengio. Show, attend and tell: Neural image caption generation with visual attention. In *International conference on machine learning*, pages 2048–2057, 2015. 2 1030
- 977 [32] Keyulu Xu, Chengtao Li, Yonglong Tian, Tomohiro Sonobe, 1031
- 978 Ken-ichi Kawarabayashi, and Stefanie Jegelka. Representation 1032
- 979 learning on graphs with jumping knowledge networks. *arXiv preprint arXiv:1806.03536*, 2018. 4 1033
- 980 [33] Zhilin Yang, Zihang Dai, Yiming Yang, Jaime Carbonell, 1034
- 981 Russ R Salakhutdinov, and Quoc V Le. Xlnet: Generalized 1035
- 982 autoregressive pretraining for language understanding. *Advances in Neural Information Processing Systems*, 32:5753– 1036
- 983 5763, 2019. 3 1037
- 984 [34] Meng Zhang, Xinchen Liu, Wu Liu, Anfu Zhou, Huadong 1038
- 985 Ma, and Tao Mei. Multi-granularity reasoning for social 1039
- 986 relation recognition from images. In *2019 IEEE International Conference on Multimedia and Expo (ICME)*, pages 1618– 1040
- 987 1623. IEEE, 2019. 2, 3, 6, 8 1041
- 988 [35] Ning Zhang, Manohar Paluri, Yaniv Taigman, Rob Fergus, 1042
- 989 and Lubomir Bourdev. Beyond frontal faces: Improving person 1043
- 990 recognition using multiple cues. In *Proceedings of the IEEE conference on computer vision and pattern recognition*, pages 4804–4813, 2015. 2, 5 1044
- 991 [36] Richard Zhang, Phillip Isola, and Alexei A Efros. Split-brain 1045
- 992 autoencoders: Unsupervised learning by cross-channel prediction. In *Proceedings of the IEEE Conference on Computer Vision and Pattern Recognition*, pages 1058–1067, 2017. 3 1046
- 993 [37] Zhanpeng Zhang, Ping Luo, Chen-Change Loy, and Xiaoou 1047
- 994 Tang. Learning social relation traits from face images. In *Proceedings of the IEEE International Conference on Computer Vision*, pages 3631–3639, 2015. 2 1048
- 995 [38] Bolei Zhou, Agata Lapedriza, Aditya Khosla, Aude Oliva, 1049
- 996 and Antonio Torralba. Places: A 10 million image database 1050
- 997 for scene recognition. *IEEE Transactions on Pattern Analysis and Machine Intelligence*, 2017. 5, 6, 8 1051
- 998 [39] Ming Tang, Mingming Fan, and Jiajun Wu. Social relation 1052
- 999 traits learning from face images. In *Proceedings of the IEEE 1053*
- 1000 Conference on Computer Vision and Pattern Recognition, pages 1054
- 1001 1058–1067, 2017. 3 1055
- 1002 [40] Ming Tang, Mingming Fan, and Jiajun Wu. Social relation 1056
- 1003 traits learning from face images. In *Proceedings of the IEEE 1057*
- 1004 Conference on Computer Vision and Pattern Recognition, pages 1058
- 1005 3631–3639, 2015. 2 1059
- 1006 [41] Ming Tang, Mingming Fan, and Jiajun Wu. Social relation 1060
- 1007 traits learning from face images. In *Proceedings of the IEEE 1061*
- 1008 Conference on Computer Vision and Pattern Recognition, pages 1062
- 1009 1068–1077, 2017. 3 1063
- 1010 [42] Ming Tang, Mingming Fan, and Jiajun Wu. Social relation 1064
- 1011 traits learning from face images. In *Proceedings of the IEEE 1065*
- 1012 Conference on Computer Vision and Pattern Recognition, pages 1066
- 1013 1071–1080, 2017. 3 1067
- 1014 [43] Ming Tang, Mingming Fan, and Jiajun Wu. Social relation 1068
- 1015 traits learning from face images. In *Proceedings of the IEEE 1069*
- 1016 Conference on Computer Vision and Pattern Recognition, pages 1070
- 1017 1075–1084, 2017. 3 1071
- 1018 [44] Ming Tang, Mingming Fan, and Jiajun Wu. Social relation 1072
- 1019 traits learning from face images. In *Proceedings of the IEEE 1073*
- 1020 Conference on Computer Vision and Pattern Recognition, pages 1074
- 1021 1079–1088, 2017. 3 1075
- 1022 [45] Ming Tang, Mingming Fan, and Jiajun Wu. Social relation 1076
- 1023 traits learning from face images. In *Proceedings of the IEEE 1077*
- 1024 Conference on Computer Vision and Pattern Recognition, pages 1078
- 1025 1085–1094, 2017. 3 1079